… to enter an enchanted world where corannulenes fall from the sky and form porous crystalline scaffolds. In their Communication on page 2195 ff., N. B. Shustova et al. merge the inherent properties of hybrid crystalline frameworks with the intrinsic properties of redox-active π-bowls for the first time. The dancing corannulene ballerinas are the opening act to the innovative corannulene science developed herein (cover design: Ekaterina A. Dolgopolova).

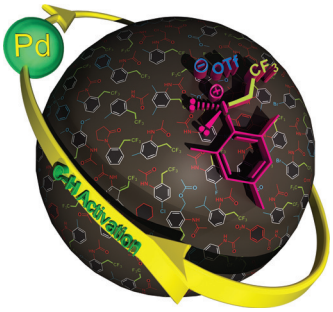

Trifluoroethylation

In their Communication on page 1988 ff., Z. Novák and co-workers describe the use of a trifluoroethyl(mesityl)iodonium salt for the simple and efficient palladium-catalyzed trifluoroethylation of aromatic compounds by C–H activation.

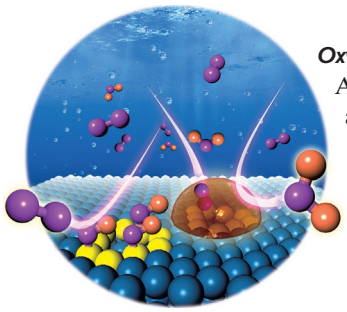

Oxygen Reduction Reaction

A hydrophobic ionic liquid protects catalytically active Pt sites from being poisoned. B. J. M. Etzold and co-workers show in their Communication on page 2257 ff. that this approach leads to dramatically boosted oxygen reduction.

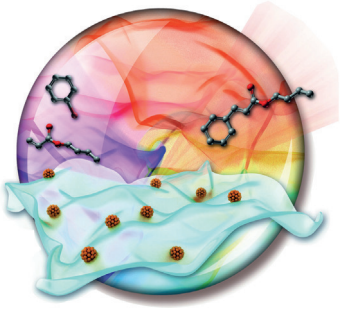

Nanosheets

In their Communication on page 2167 ff., Y. Yin, T. Zhang, et al. show how transition-metal hydroxide nanosheets less than 5 nm thick can be modified to form highly active Heck reaction catalysts.

How to contact us:

Editorial Office:
E-mail: angewandte@wiley-vch.de
Fax: (+49) 62 01–606-331
Telephone: (+49) 62 01–606-315

Reprints, E-Prints, Posters, Calendars:
Carmen Leitner
E-mail: chem-reprints@wiley-vch.de
Fax: (+49) 62 01–606-331
Telephone: (+49) 62 01–606-327

Copyright Permission:
Bettina Loycke
E-mail: rights-and-licences@wiley-vch.de
Fax: (+49) 62 01–606-332
Telephone: (+49) 62 01–606-280

Online Open:
Margitta Schmitt
E-mail: angewandte@wiley-vch.de
Fax: (+49) 62 01–606-331
Telephone: (+49) 62 01–606-315

Subscriptions:
www.wileycustomerhelp.com
Fax: (+49) 62 01–606-184
Telephone: 0800 1800536 (Germany only)
+44(0) 1865476721 (all other countries)

Advertising:
Marion Schulz
E-mail: mschulz@wiley-vch.de
Fax: (+49) 62 01–606-550
Telephone: (+49) 62 01–606-565

Courier Services:
Boschstrasse 12, 69469 Weinheim

Regular Mail:
Postfach 101161, 69451 Weinheim

Angewandte Chemie International Edition is a journal of the Gesellschaft Deutscher Chemiker (GDCh), the largest chemistry-related scientific society in continental Europe. Information on the various activities and services of the GDCh, for example, cheaper subscription to *Angewandte Chemie International Edition*, as well as applications for membership can be found at **www.gdch.de** or can be requested from GDCh, Postfach 900440, D-60444 Frankfurt am Main, Germany.

GDCh
Gesellschaft Deutscher Chemiker

Service

Author Profile

"In a spare hour, I enjoy a good glass of red wine and Bill Evans.
My biggest inspiration is my family. …"
This and more about Haoshen Zhou can be found on page 1956.

News


W. R. Dichtel


P. Yang


J.-P. Stasch


A. R. Fout


K. R. M. Mackey


K. N. Parent


L. Whittaker-Brooks


M. Antonietti

Books

Highlights

Aromaticity

The lightest synthetically accessible Hückel π-aromatic system, a triboracyclopropenyl dianion bearing three dicyclohexylamino groups, has been obtained by reduction of dicyclohexylaminoboron dichloride and structurally characterized as the dimeric disodium salt (see scheme; Cy = cyclohexyl, DME = 1,2-dimethoxyethane).

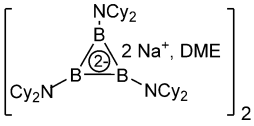

Minireviews

Medicinal Chemistry

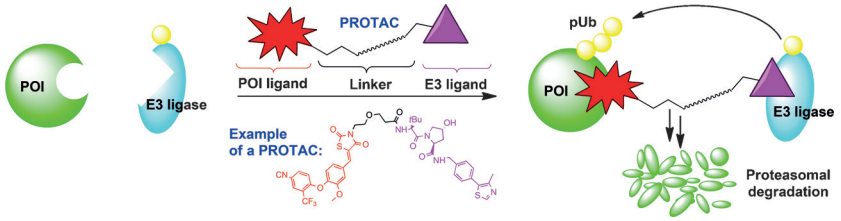

Now we're just falling apart: The use of small-molecule proteolysis-targeting chimeras (PROTACs) to induce protein degradation offers an alternative therapeutic strategy to the traditional inhibitor-based approach. Recent progress in developing small-molecule PROTACs to mediate the proteasomal degradation of targeted proteins is presented, and the opportunities and challenges of this technology for drug discovery are discussed.

Reviews

Molecular Recognition

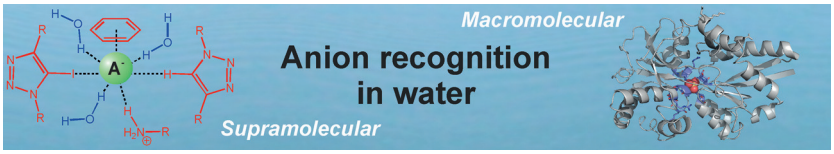

The quest for recognition: The recognition of anions in water is a great challenge for supramolecular chemistry. Recently, great strides have been made in this area by exploiting exotic interactions such as C–H hydrogen bonding and halogen bonding, as well as exercising control over the hydrophobic effect. Recognition strategies based on biomolecules, polymers, and nanoparticles also offer a complementary approach to anion binding in the aqueous phase.

For the USA and Canada: ANGEWANDTE CHEMIE International Edition (ISSN 1433-7851) is published weekly by Wiley-VCH, PO Box 101161, 69451 Weinheim, Germany. US mailing agent: SPP, PO Box 437, Emigsville, PA 17318. Periodicals postage paid at Emigsville, PA. US POSTMASTER: send address changes to *Angewandte Chemie*, John Wiley & Sons Inc., C/O The Sheridan Press, PO Box 465, Hanover, PA 17331. Annual subscription price for institutions: US$ 16.862/14.051 (valid for print and electronic / print or electronic delivery); for individuals who are personal members of a national chemical society prices are available on request. Postage and handling charges included. All prices are subject to local VAT/sales tax.

Communications

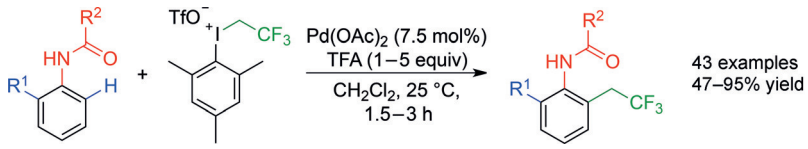

Trifluoroethylation

Simple: Anilides can be trifluoroethylated with a 2,2,2-trifluoroethyl-substituted iodonium salt in the presence of a palladium catalyst under mild conditions (see scheme). The reaction proceeds by C–H activation at the *ortho* position and features a broad substrate scope.

Frontispiece

Reversible G-quadruplex pH switch: A human telomere DNA sequence has been found to adopt two distinct two G-quartet antiparallel basket-type G-quadruplexes, a TD and KDH$^+$ form, which can reversibly transform to each other by variation of pH. The protonation and deprotonation of A20 is the key for the transformation. Reversibility offers possibilities for its utilization as conformational switch in a highly polymorphic system.

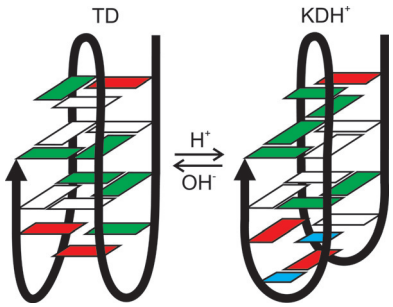

G-Quadruplexes

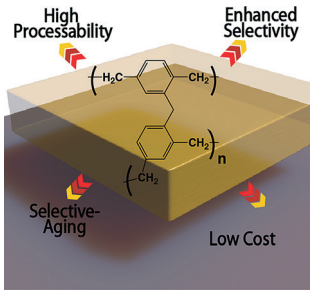

Giving membranes eternal youth: Preventing the collapse of pores in gas-separation membranes vastly improves their lifetime. In fact, the high performance membranes improve with age. The hypercrosslinked polymer additive used for this is cheap to manufacture and has very high processability. This brings the reality of high-performance membranes in the market much closer.

Gas-Separation Membranes

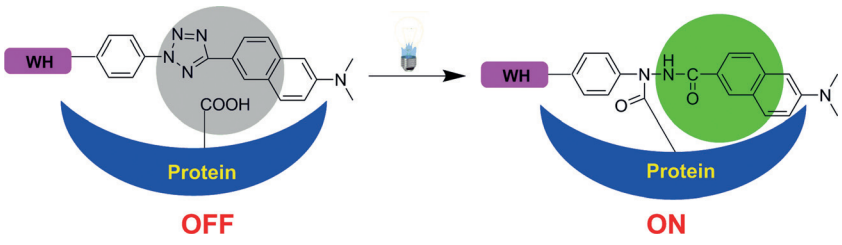

"Tie" and "see": By reassessing the bioorthogonality of tetrazole photoclick chemistry, an alternative use of tetrazoles in chemical biology is proposed, as general photo-crosslinkers with potential fluorescence Turn-ON properties. This method could be used to develop affinity-based probes for live-cell imaging of endogenous kinase activities. WH = warhead.

Photoclick Chemistry

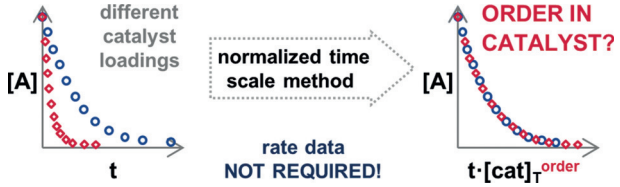

A graphical analysis to elucidate the order in catalyst uses a normalized time scale, $t[cat]_T^n$, to adjust entire reaction profiles constructed with concentration data. Compared to methods that use rates, the normalized time scale analysis requires fewer experiments and minimizes the effects of experimental errors by using information on the entire reaction profile.

Kinetic Analysis

Tricky Teflon: The use of Teflon in making mesostructured carbon materials eliminates toxic HF handling and shortens the synthesis time. Silica template removal and carbonization are combined into a single step. The obtained carbon JNC-1 has a higher surface area (see picture) and pore volume compared to conventionally obtained carbons (such as CMK-3) via the HF etched route.

Mesoporous Materials

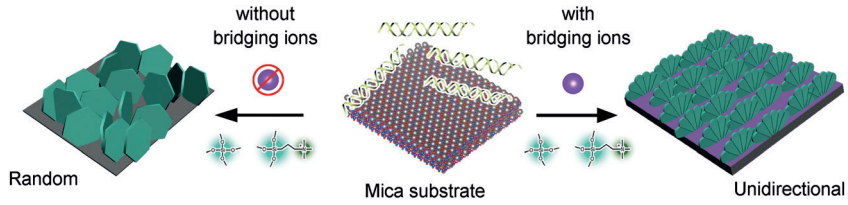

An oriented chiral DNA–silica film was fabricated using crystalline mica as both substrate and template. The connecting effect of the bridging metal ions between DNA molecules and the substrate led to vertical growth of chiral blades and alignment of the film in uniform horizontal direction. This coincides with the crystal orientation of the mica surface, producing a large-scale chiral film with long-range alignment.

Chiral Films

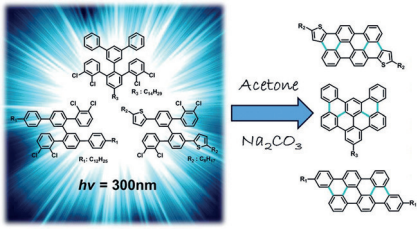

Gently does it: Upon irradiation under metal-free, mild conditions, chlorinated precursors underwent up to four regioselective cyclization reactions to provide rigid π-conjugated molecules (see example). This photochemical cyclodehydrochlorination reaction was compatible with both electron-poor and electron-rich substrates, thus enabling the synthesis of pyridine- and thiophene-fused nanographenes.

Carbon Materials

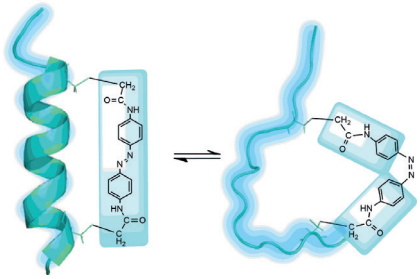

Using quantum mechanics/molecular mechanics (QM/MM) and classical MM dynamics methods the photoinduced folding and unfolding of an azobenzene cross-linked peptide was simulated. The interaction between the peptide and the cross-linker plays a key role not only in regulating the photoinduced evolution of the secondary structure of the peptide, but also in tuning the photoisomerization mechanism of the azobenzene cross-linker.

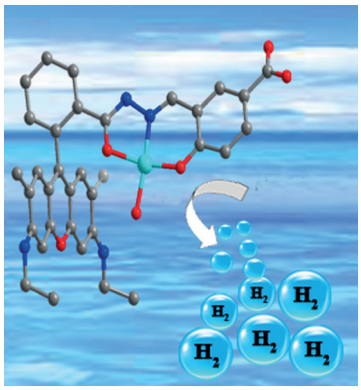

On active duty: High activity for the generation of hydrogen has been found on irradiating a crystalline coordination polymer containing redox-active copper centers and rhodamine-derived organic linkers with visible light. The ordered stacking of the linkers induced rapid transfer of photogenerated electrons to the copper nodes, which have open coordination sites and a favorable redox potential for reducing protons to dihydrogen.

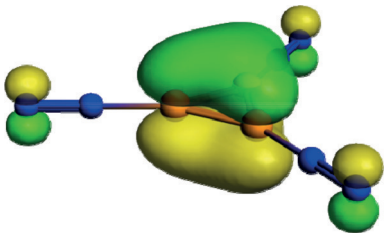

Minimal π systems: The $[B_3(NN)_3]^+$ and $[B_3(CO)_3]^+$ complexes are identified through infrared photodissociation spectroscopy. The complexes feature the smallest π-aromatic system B_3^+. Quantum chemical bonding analysis reveals that the adducts are stabilized by L→$[B_3L_2]^+$ σ-donation.

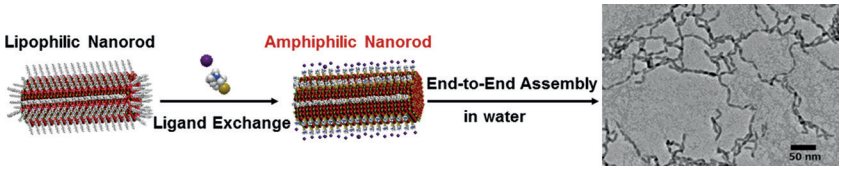

Falling into line: The exchange of alkylphosphonic acid ligands on wurtzite CdSe nanorods for short-chained water-soluble thiols rendered the surface of the nanorods amphiphilic in nature. The amphiphilic nanorods self-assembled into one-dimensional nanowires through hydrophobic end-to-end interactions in water. CdSe tetrapods were incorporated into the self-assemblies as branching points.

Nucleic Acid Detection

ATP lighting the way: Chimeric dinucleotides were designed to release ATP during polymerase-mediated synthesis of DNA. This ATP can be used to generate a signal with luciferase, thereby allowing the sensitive isothermal detection of both large (phage DNA) and small (miRNA) nucleic acids.

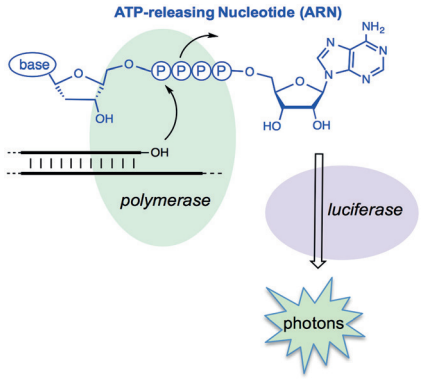

Hydrogels

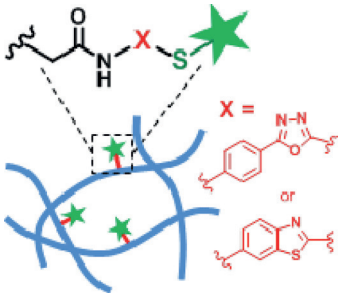

Methylsulfonyl polyacrylamide (P(AAm) gels allow easy, specific, and functional covalent coupling of thiol-containing ligands in tunable concentrations under physiological conditions, while retaining the same swelling, porosity, cytocompatibility, protein repellance, and tunable stiffness of P(AAm) gels.

Phase Transitions

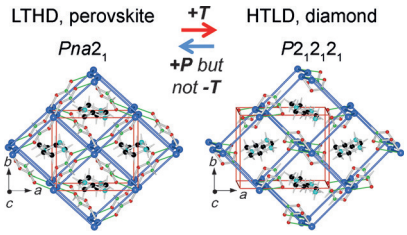

$[CH_3CH_2NH_3][Cu(HCOO)_3]$ shows a phase transition from low-temperature high-density (LTHD) perovskite to high-temperature low-density (HTLD) diamond by heating, but the backward transition can only be induced by pressure. The copper–formate bond rearrangement, a bridging-chelating switch of formate, changes in N–H···O H-bonds, and flipping of ethylammonium are involved in the transition.

Antitumor Agents

Amorphous iron nanoparticles (AFeNPs) can be used for cancer theranostics. Ionization of the AFeNPs in the mildly acidic tumor microenvironment promotes the release of ferrous ions in the tumor; these induce H_2O_2 disproportionation, which in turn leads to efficient $^{\bullet}OH$ generation and significant tumor growth inhibition.

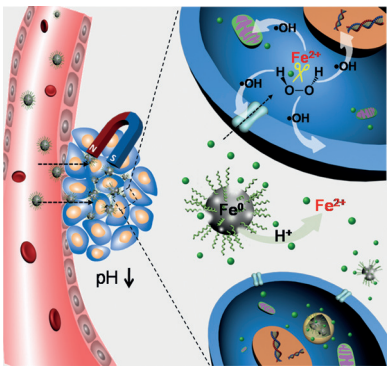

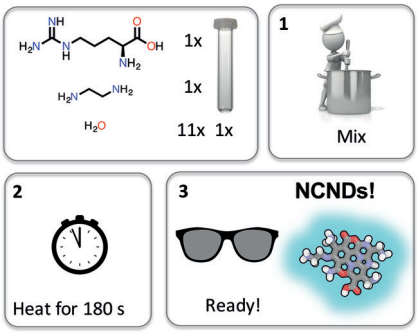

Fluorescent nanodots: A simple and controllable bottom-up route to size- and surface-controllable nitrogen-doped carbon nanodots (NCNDs) under microwave irradiation is reported. These NCNDs are among the smallest nanodots reported so far, with some of the highest quantum yields.

Carbon Nanodots

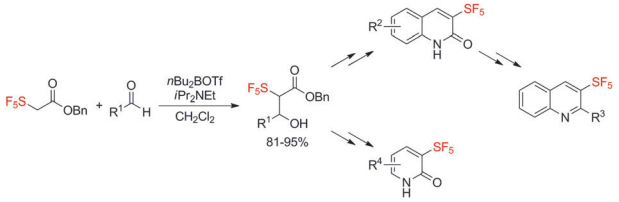

Easy SF_5 installation: Enolate in α-position of a pentafluorosulfanyl group was generated and underwent aldol reaction to give SF_5-heterocycles in excellent yields. Comparison of their physicochemical data with those of their trifluoromethyl and *tert*-butyl analogues confirmed that the SF_5 group can be considered as a surrogate for CF_3 and *t*-Bu groups with potential fine-tuning effects.

Heterocycles

Two-faced therapeutics: Octopus-type PEG-Au-PAA/$mSiO_2$-LA Janus NPs are fabricated with pH and NIR light dual-stimuli responsive properties and targeting specificity for synergistic chemo-photothermal cancer therapy in vitro and in vivo.

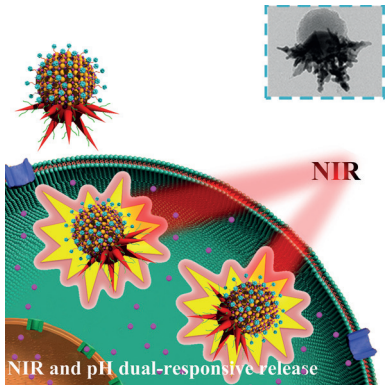

Drug Delivery

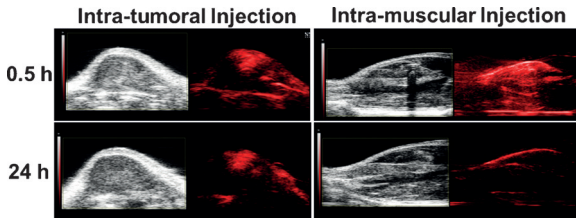

A photothermal nanoagent has been developed, namely degradable PEGylated molybdenum oxide, with strong near-IR absorbance, high drug loading capability, and pH-dependent degradation. It can be rapidly excreted from the body after intravenous injection and shows no appreciable in vivo toxicity. It also shows effective accumulation and retention in the tumor, which can then be eliminated by photothermal therapy treatment.

Photothermal Therapy

Dynamic Materials

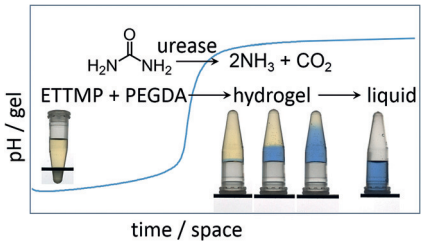

In control at the front line: By coupling a base-catalyzed thiol-Michael addition with a base-producing autocatalytic enzyme reaction, it was possible to program gelation and generate propagating polymerization fronts (see picture; ETTMP is a polymeric trithiol, PEGDA is poly(ethylene glycol) diacrylate). The rate of hydrolytic degradation of the resulting hydrogel depended on the initial concentrations of the components of the system.

Photoswitches

Global refolding of a helical foldamer is induced by a change in pH or by photochemically induced transamidation. As a result, information about a single local hydrogen bond is transmitted to a remote catalytically active site, and translated into a switch in conformation that reverses the enantioselectivity of its reactions.

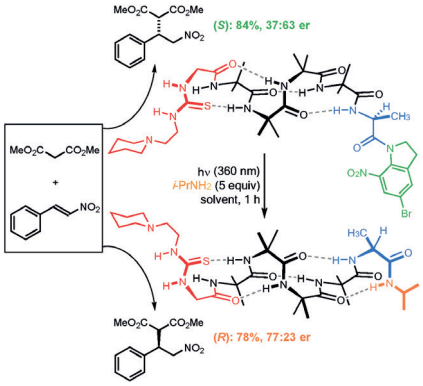

Hydrogen Evolution

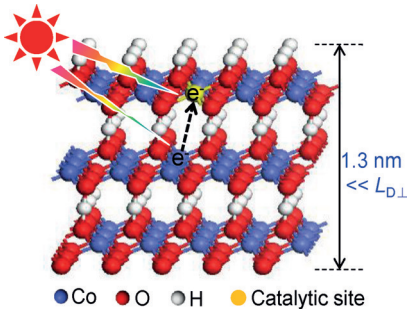

The thickness of a layered β-CoOOH semiconductor was reduced to obtain an atomically thin two-dimensional nanostructure. Electron–hole recombination is almost suppressed in the 1.3 nm thick β-CoOOH nanosheet, which leads to excellent electron–hole separation efficiencies and superior hydrogen production rates ($L_{D\perp}$: carrier diffusion length along the *c* axis).

Biosynthesis

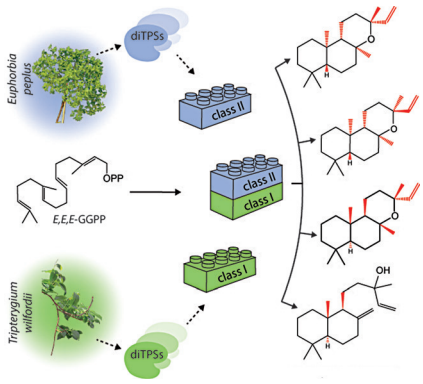

Beyond the horizon: A broad range of cyclic diterpenes, including precursors for therapeutic compounds, was efficiently biosynthesized by combining class I and II diterpene synthase enzymes from diverse species. Stereospecific cyclizations were achieved and scale-up was demonstrated with efficient biotechnological production.

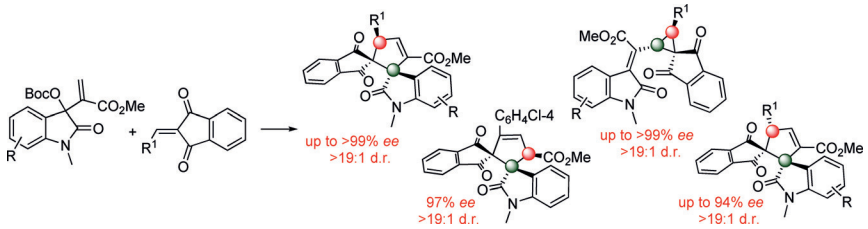

Switching it up: The title reactions have been accomplished by employing different chiral Lewis base catalysts, thus resulting in a broad collection of chiral compounds with high structural and stereochemical diversity (see scheme). DFT calculations indicate that the structure of Lewis base plays a key role in controlling the chemo- and diastereoselectivity. Boc = *tert*-butoxycarbonyl.

Organocatalysis

Caged siRNAs with a single photolabile linker and/or vitamin E modification at 5′ terminal were rationally designed and synthesized. These virtually inactive caged siRNAs could be fully restored to native siRNAs through simple light activation with up to an 18.6-fold enhancement of gene silencing activity.

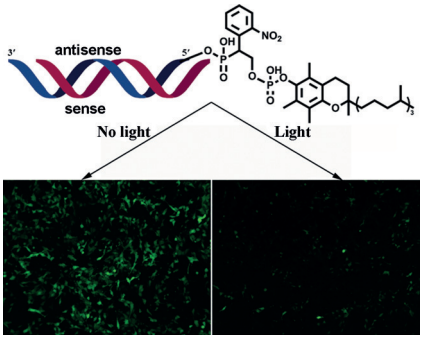

Gene Regulation

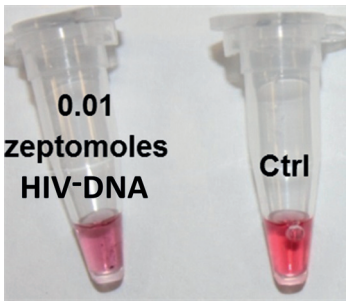

Goodbye gels! PCR developer is a rapid (5 min), highly specific, and universal naked-eye assay to replace gel electrophoretic analysis of PCR reactions.

Analytical Methods

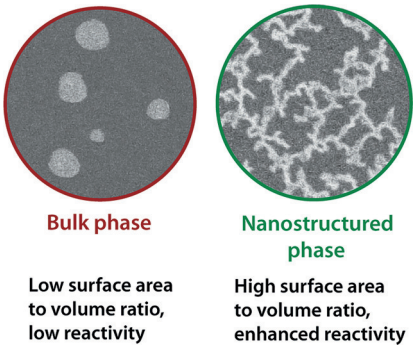

Watered down: The formation of micrometer- and nanometer-scale compartments in ionic liquids, mediated by addition of water, can be directly observed by using electron microscopy. The morphologies, which include isolated droplets, aggregates, and 2D meshworks, change according to the amount of added water. The ionic liquid/water systems were applied to the formation of the platform chemical 5-(hydroxymethyl)furfural.

Ionic Liquids

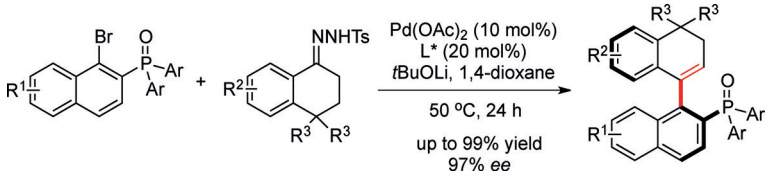

With a twist: An enantioselective palladium-catalyzed synthesis of atropisomeric vinyl arenes from aryl bromides and hydrazones is reported. The use of hydrazone precursors as coupling partners resulted in mild reaction conditions, and thus a broad functional-group tolerance. The products were isolated with *ee* values of up to 97%. Ts = 4-toluenesulfonyl.

Biaryls

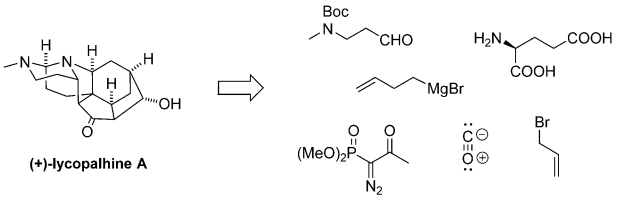

Just Another Mannich Monday: By using L-glutamate and L-proline as a starting material and catalyst, respectively, the complex alkaloid lycopalhine A was assembled in only 13 steps. The synthesis features not only an unusual Mannich reaction but also a biomimetic aldol addition that completes the intricate carbon skeleton of the natural product.

Natural Product Synthesis

Where is the corannulene? A porous crystalline hybrid scaffold with immobilized redox-active corannulene buckybowls has been prepared. The scaffold combines the periodicity, dimensionality, and structural modularity of hybrid frameworks with the intrinsic properties of redox-active π-bowls.

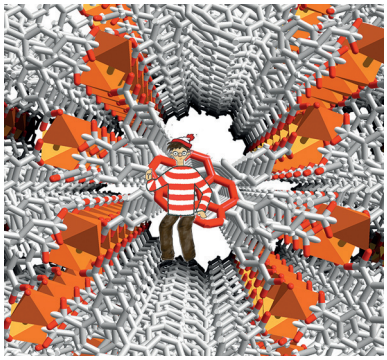

Hybrid Materials

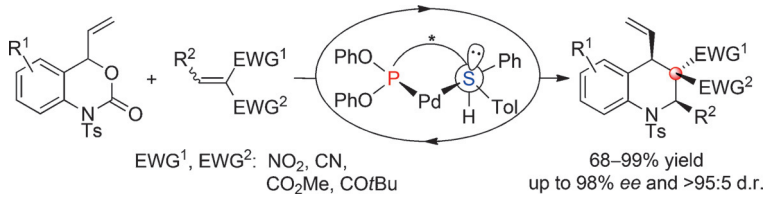

Hybrid ligands: By combining a chiral β-amino sulfide and a simple diphenyl phosphite, a new hybrid P,S ligand was used for title reaction. By doing so, multiple contiguous stereocenters and a chiral quaternary center were rapidly constructed and highly functionalized tetrahydroquinolines were produced in up to 99% yield with 98% *ee* and greater than 95:5 d.r.

Ligand Design

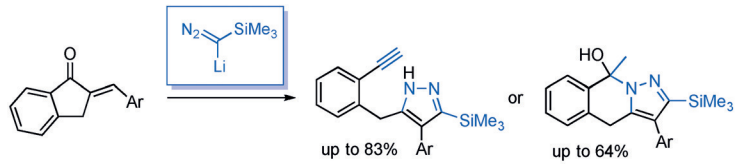

The sequential 1,4-/1,2-addition of lithium(trimethylsilyl)diazomethane to cyclic α,β-unsaturated ketones induces various subsequent transformations, such as Grob-type C–C fragmentation or alkylidene carbene mediated Li–N insertion, depending on the ring size and the position of the double bond. Various nitrogen heterocycles were thus obtained in good yields.

C–C Bond Fragmentation

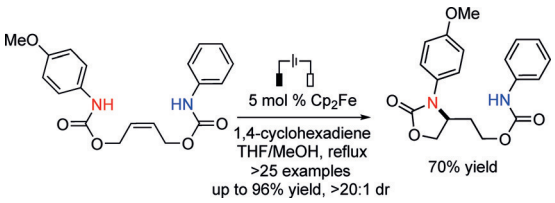

Easy access to *N*-arylamidyl radicals: The first electrocatalytic method for the generation of amidyl radicals from anilides has been developed using ferrocene (Cp_2Fe) as a highly reactive, yet chemoselective redox catalyst. Based on this radical-generating method, a highly chemo- and diastereoselective olefin hydroamidation reaction has been developed.

Organic Electrochemistry

Double function: Nitrogen- and phosphorus-codoped 3D graphitic carbon networks were generated by self-assembling melamine and phytic acid into supermolecular aggregates in the presence or absence of graphene oxide, followed by pyrolysis. They display remarkably high bifunctional electrocatalytic activities for both oxygen reduction and hydrogen evolution reactions.

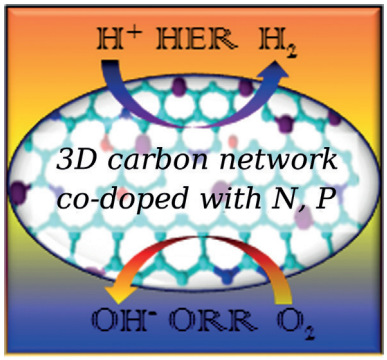

Electrocatalysis

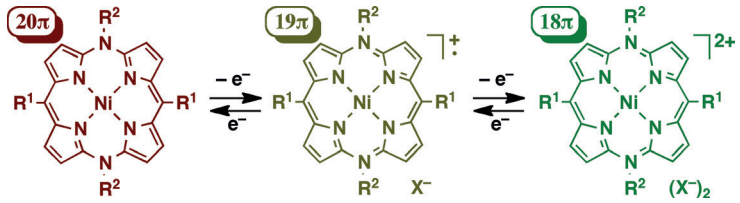

N makes all the difference: Redox-switchable 20π-, 19π-, and 18π-electron 5,10,15,20-tetraaryl-5,15-diazaporphyrinoids are prepared through metal-templated annulation of Ni^{II} bis(dipyrrin) complexes followed by oxidation. The *meso* N atoms in these diazaporphyrinoids give rise to characteristic redox and optical properties for the compounds that are not typical of isoelectronic 5,10,15,20-tetraarylporphyrins.

Porphyrinoids

Photochemistry

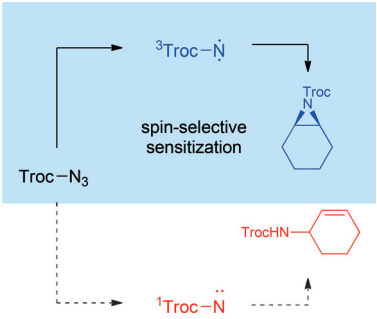

A fresh spin on heterocycles: Synthetically useful photochemical aziridinations can be achieved by using a visible-light-activated transition-metal photosensitizer to produce nitrenes exclusively in their triplet spin state. A wide range of aliphatic and aromatic alkenes can be readily aziridinated without competitive allylic insertion reactions. TrocN$_3$ = 2,2,2-trichloroethyl azidoformate.

Synthetic Methods

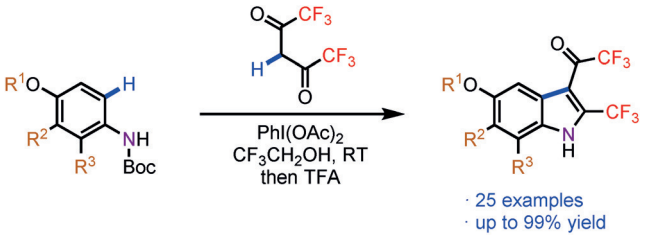

A telescoped synthesis: In the title reaction, N-Boc anilines are reacted with hexafluoroacetylacetone in presence of phenyliodine(III) diacetate followed by trifluoroacetic acid (TFA) to yield fluorinated indoles in a single pot. Additionally, the versatility of the trifluoroacetyl group is exploited through ketone-like and ester-like chemistry.

Aminohydroxylation

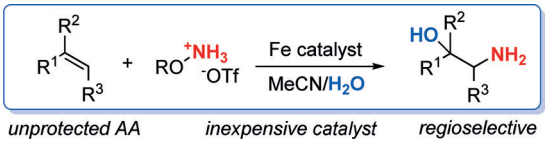

With an iron hand: Aryl-substituted amino alcohols are privileged scaffolds in medicinal chemistry and natural products. An exceptionally simple and inexpensive Fe^{II} complex can efficiently catalyze the direct transformation of simple alkenes into unprotected amino alcohols in good yield and perfect regioselectivity. This new catalytic method was applied in the expedient synthesis of bioactive molecules and could be extended to aminoetherification.

Enzyme Ligands

A new probe for drug design: An affinity probe for Sirt2 has been developed that shows excellent selectivity and potency. The slow dissociation rate of the enzyme–ligand complex enables new applications, such as biolayer interferometry, and pull-down assays for sirtuin rearranging ligands.

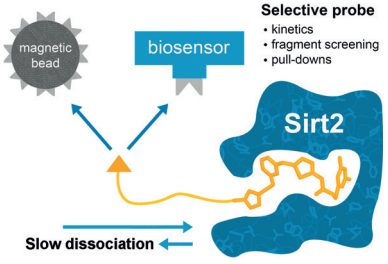

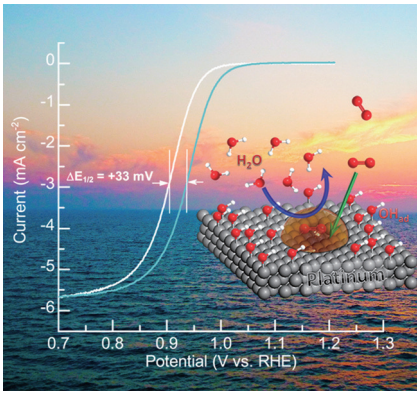

Keep my place: A hydrophobic ionic liquid phase helps protect the Pt sites from being poisoned by nonreactive oxygenated species, leading to dramatically improved kinetics of the oxygen reduction reaction (ORR) on platinum catalyst.

Oxygen Reduction

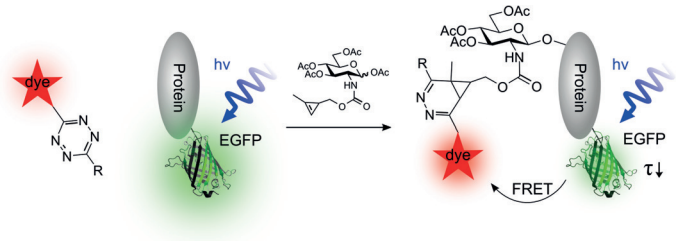

Living proof: Protein-specific glycosylation inside living cells was imaged by detecting FRET between an EGFP fused to the protein of interest and a fluorophore ligated to a metabolically incorporated *N*-acetylglucosamine derivative through an inverse-electron-demand Diels–Alder reaction. FRET can be detected with high contrast even in presence of a large excess of acceptor fluorophores by fluorescence lifetime imaging microscopy (FLIM).

Glycoproteins

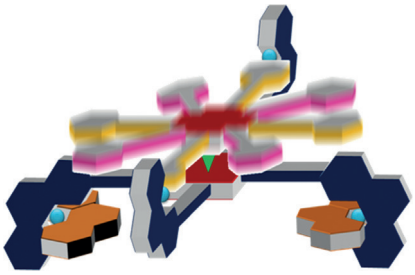

The magic self-assembly of supramolecular machinery! When five components are mixed, supramolecular rotors form, which depending on the fifth component (= brake block) exhibit different rotational frequencies that are quantitatively predictable.

Nanorotors

Supporting information is available on www.angewandte.org (see article for access details).

A video clip is available as Supporting Information on www.angewandte.org (see article for access details).

This article is available online free of charge (Open Access).

This article is accompanied by a cover picture (front or back cover, and inside or outside).

The Very Important Papers, marked VIP, have been rated unanimously as very important by the referees.

The Hot Papers are articles that the Editors have chosen on the basis of the referee reports to be of particular importance for an intensely studied area of research.

Angewandte Corrigendum

Rhodium-Catalyzed Asymmetric Synthesis of Spirosilabifluorene Derivatives

Y. Kuninobu,* K. Yamauchi, N. Tamura, T. Seiki, K. Takai* **1520–1522**

Angew. Chem. Int. Ed. **2013**, *52*

DOI: 10.1002/anie.201207723

The *R* and *S* designations for the absolute configuration of the chiral spirosilabifluorenes were incorrectly assigned in the Communication. As shown by the single-crystal X-ray analysis results in Figure 1, the absolute configuration of the major enantiomers from the reaction with [{RhCl(cod)}$_2$] and (*R*)-binap were "*R* form" not "*S* form". Table 1 and the sentences in the original manuscript should be revised as follows:

page 1520, right column, Table 1: "*R*" as the major enantiomer for entries 1 and 4
page 1520, line 11 of the right column: "... the *R* form (Figure 1 and the Supporting ..."
page 1521, line 2 of the left column: "... preparation of **2e** from (*R*)-**2b** (See ..."
page 1521, line 6 of the left column: "compound derived from (*R*)-**2b** on"
page 1522, Ref. [8]: "... gave (−)-(*S*)-**2b** in 95% yield, 81% *ee*."
page 1522, Ref. [9]: "... eluent)]; time: *S* form, 23 min; *R* form, 24.5 min}"
page 1522, Ref. [12]: "... by preparation of (*R*)-**2e** from (*R*)-**2b**. The details ..."
page 1522, Ref. [13]: "CCDC 914745 [(*R*)-**2b**] contains the ...}"

The absolute configurations for spirosilabifluorenes **2b** and **2e** in the Supporting Information (page S6) should be corrected to "*R*" in the same way. In addition, graphics for spirosilabifluorenes **2b**–**2f** in the Supporting Information (pages S4 and S5) contain several errors as well. The corrected figures are shown below:

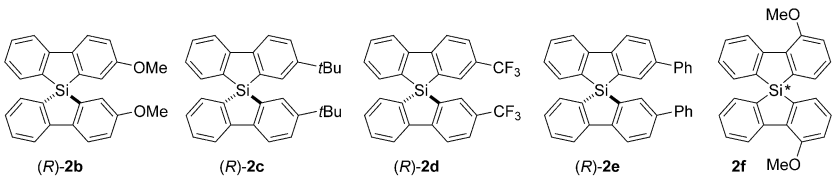

Although the absolute configuration of **2c**, **2d**, and **2f** was not determined in 2012, the *R* configuration has recently been confirmed for **2c** and **2d** using single-crystal X-ray diffraction.
The mistakes regarding the absolute configurations do not affect the validity of any of the reported yields, data, ORTEP drawings, or information provided in the experimental sections of the original manuscript and the Supporting Information. In addition, the results and conclusions of the Communication also remain valid.
The authors sincerely apologize for the errors in reporting the configurations.

Angewandte Addendum

In this Communication, the authors reported the crystal structure of the glyoxal bis(amidiniumhydrazone) (GBAH) sulfate salt, whose synthesis was first reported by Thiele and Dralle in 1898.[1] The structure showed the sulfate crystallized as extended $[SO_4(H_2O)_5^{2-}]_n$ clusters. As an important part of this study, it was demonstrated for the first time that competitive crystallization of GBAH sulfate from aqueous solutions can be used as a basis for selective sulfate separation. The effectiveness of this crystallization-based sulfate separation method stems from the relatively low aqueous solubility of GBAH sulfate ($K_{sp} = 3.2 \times 10^{-7}$),[2] comparable with that of $SrSO_4$.
In the interest of completeness, the authors note that observations of the relatively insoluble nature of the sulfate salts of GBAH or other analogs had been previously made,[3] though no solubility values had been reported. Single-crystal X-ray structural studies of GBAH analogues showed that the sulfate anion can crystallize with variable numbers of water molecules (from zero to six).[4] However, due to the limited structural and solubility data available, it is not clear at this point the extent to which the included water molecules contribute to the low solubility of these salts and to the sulfate crystallization selectivity. Future structure–solubility relationship studies of bis(amidiniumhydrazone) sulfate salts offer the prospect for understanding the various factors controlling the crystallization efficiency of this intriguing class of compounds.[5]

[1] J. Thiele, E. Dralle, *Justus Liebigs Ann. Chem.* **1898**, *302*, 275.
[2] The solubility product was calculated from the measured solubility of GBAH sulfate of 7.2 $\times 10^{-4}$ M, and taking into account the corresponding activity coefficient of 0.78, estimated by the Debye–Huckel limiting law.
[3] a) P. Seppanen, R. Fagerstrom, L. Alhonen-Hongisto, H. Elo, P. Lumme, J. Janne, *Biochem. J.* **1984**, *221*, 483; b) H. Elo, *Spectroscopy Lett.* **1989**, *22*, 123; c) H. Elo, *Spectroscopy Lett.* **1989**, *22*, 161.
[4] a) P. O. Lumme, I. Mutikainen, H. O. Elo, Acta Cryst. **1986**, C*42*, 1209; b) H. Elo, I. Mutikainen, L. Alhonen-Hongisto, R. Laine, J. Jänne, P. Lumme, *Z. Naturforsch.* **1986**, *41c*, 851; c) H. Elo, I. Mutikainen, *Z. Naturforsch.* **1988**, *43c*, 601; d) M. Koskinen, I. Mutikainen, H. Elo, *Z. Naturforsch.* **1996**, *51b*, 1161; e) M. Koskinen, I. Mutikainen, J. T. Koskinen, H. Elo, *Z. Naturforsch.* **1997**, *52b*, 1114.
[5] R. Custelcean, N. J. Williams, C. A. Seipp, A. S. Ivanov, V. S. Bryantsev, *Chem. Eur. J.* DOI: 10.1002/chem.201504651.

Angewandte Corrigendum

In this Communication, an affiliation needs to be added for one of the authors.

[e] Prof. C. Rovira
Institució Catalana de Recerca i Estudis Avançats (ICREA), Passeig Lluís Companys, 23, 08010 Barcelona (Spain)

